Journal of Ecology

Journal of Ecology doi: 10.1111/1365-2745.12770

Soil carbon response to woody plant encroachment: importance of spatial heterogeneity and deep soil storage

Yong Zhou*, **Thomas W. Boutton** and **X. Ben Wu**

Department of Ecosystem Science and Management, Texas A&M University, College Station, TX 77843, USA

Summary

1. Recent global trends of increasing woody plant abundance in grass-dominated ecosystems may substantially enhance soil organic carbon (SOC) storage and could represent a strong carbon (C) sink in the terrestrial environment. However, few studies have quantitatively addressed the influence of spatial heterogeneity of vegetation and soil properties on SOC storage at the landscape scale. In addition, most studies assessing SOC response to woody encroachment consider only surface soils, and have not explicitly assessed the extent to which deeper portions of the soil profile may be sequestering C.

2. We quantified the direction, magnitude and pattern of spatial heterogeneity of SOC in the upper 1·2 m of the profile following woody encroachment via spatially specific intensive soil sampling across a landscape in a subtropical savanna in the Rio Grande Plains, USA, that has undergone woody proliferation during the past century.

3. Increased SOC accumulation following woody encroachment was observed to considerable depth, albeit at reduced magnitudes in deeper portions of the profile. Overall, woody clusters and groves accumulated 12·87 and 18·67 Mg C ha^{-1} more SOC compared to grasslands to a depth of 1·2 m.

4. Woody encroachment significantly altered the pattern of spatial heterogeneity of SOC to a depth of 5 cm, with marginal effect at 5–15 cm, and no significant impact on soils below 15 cm. Fine root density explained greater variability of SOC in the upper 15 cm, while a combination of fine root density and soil clay content accounted for more of the variation in SOC in soils below 15 cm across this landscape.

5. *Synthesis.* Substantial soil organic carbon sequestration can occur in deeper portions of the soil profile following woody encroachment. Furthermore, vegetation patterns and soil properties influenced the spatial heterogeneity and uncertainty of soil organic carbon in this landscape, highlighting the need for spatially specific sampling that can characterize this variability and enable scaling and modelling. Given the geographic extent of woody encroachment on a global scale, this undocumented deep soil carbon sequestration suggests this vegetation change may play a more significant role in regional and global carbon sequestration than previously thought.

Key-words: δ^{13}C value, deep soil carbon, landscape scale, pattern of spatial heterogeneity, plant–soil (below-ground) interactions, SOC storage, subtropical savanna, woody plant encroachment

Introduction

Grass-dominated ecosystems in arid and semi-arid regions around the world have experienced increased woody plant abundance during the past century (Van Auken 2000, 2009; Eldridge *et al.* 2011; Stevens *et al.* 2017). This globally widespread phenomenon has dramatically altered the structure and function of grassland and savanna ecosystems (Maestre *et al.* 2009; Eldridge *et al.* 2011), with the potential to profoundly influence grassland biodiversity (Ratajczak, Nippert & Collins 2012), hydrology (Huxman *et al.* 2005), biogeochemistry (Boutton, Archer & Midwood 1999; Hibbard *et al.* 2003; Chiti *et al.* 2017) and livestock production (Dalle, Maass & Isselstein 2006). As arid and semi-arid systems occupy more than 40% of Earth's land surface (Bailey 1996),

*Correspondence author. E-mail: zhouyong1222@tamu.edu

a shift from grass-dominated to woody-dominated ecosystems could potentially influence the global carbon (C) cycle and the climate system via the impacts on soil organic carbon (SOC) stocks and dynamics.

Land cover change is often associated with a change in C stocks (Guo & Gifford 2002; Don, Schumacher & Freibauer 2011; Pellegrini, Hoffmann & Franco 2014). The encroachment of woody plants into grasslands/savannas has been considered to be a potentially large C sink at regional and global scales due to the accumulation of C in both biomass and soils (Pacala *et al.* 2001; King *et al.* 2007; Dean *et al.* 2015). However, at the ecosystem level, the effects of woody encroachment on SOC stocks are often equivocal, with studies showing increased SOC stocks in some ecosystems (Schlesinger *et al.* 1996; Maestre *et al.* 2009; Liu *et al.* 2011; Blaser *et al.* 2014), no net change (Hughes *et al.* 2006) and reductions in others (Jackson *et al.* 2002; Oelofse *et al.* 2016). Reasons for these inconsistencies still remain unknown, but may be ascribed to soil characteristics and historical land use patterns (Jackson *et al.* 2002; Barger *et al.* 2011; Li *et al.* 2016), or the lack of appropriate methodology for estimating SOC stocks in encroached systems with complex vegetation patterns (Throop & Archer 2008; Liu *et al.* 2011). In addition, most of these studies have evaluated the impact of woody encroachment only on surficial SOC stocks (down to 30 cm at most, IPCC recommended sampling depth; IPCC, 2006) (e.g. Hughes *et al.* 2006; Maestre *et al.* 2009; Liu *et al.* 2011; Blaser *et al.* 2014), and few studies have examined SOC accumulation in deeper soil layers (below 30 cm) (Boutton, Archer & Midwood 1999; Jackson *et al.* 2002; Chiti *et al.* 2017). Compared to herbaceous species, trees/shrubs typically have much deeper rooting systems (Jackson *et al.* 1996; Schenk 2006; Yang, Donohue & McVicar 2016). The allocation of C to deep roots by encroaching woody plants, as the major source of C input in subsoil (Rumpel & Kögel-Knabner 2011), may be expected to increase SOC accumulation in deeper soil layers. On the other hand, deep roots may prime the decomposition of otherwise stable subsurface SOC through the addition of labile root C (e.g. Fontaine *et al.* 2007; Mobley *et al.* 2015). Therefore, the direction and magnitude of SOC stocks response to woody encroachment in deeper portions of the soil profile remain largely unknown, and study of deep soil is crucial for understanding SOC dynamics and for making robust predictions of terrestrial C budgets following vegetation cover change.

Woody encroachment into grass-dominated ecosystems may also increase the spatial heterogeneity of soil properties (e.g. islands of fertility, Schlesinger *et al.* 1996), making it more difficult to accurately quantify ecosystem properties and processes based on micro-sites and limited sample size (Throop & Archer 2008; Liu *et al.* 2011). Previous studies have demonstrated the value of quantifying spatial patterns of soil properties and associated variability to study-related processes in arid and semi-arid regions with patchy vegetation (Schlesinger *et al.* 1996; Throop & Archer 2008; Bai *et al.* 2009; Liu *et al.* 2011; Daryanto, Eldridge & Wang 2013b), but their results were restricted to the topsoil (0–20 cm). Woody encroachment has been confirmed to substantially alter the spatial pattern and variability of SOC in topsoil at the individual woody patch scale from bole to the perimeter (Throop & Archer 2008) and at the landscape scale where the landscape comprises different sizes of woody patches (Liu *et al.* 2011). To our knowledge, however, no study has explicitly assessed the extent to which woody encroachment alters the spatial pattern of SOC in deeper portions of the soil profile. Non-spatial soil core studies suggest that deeper SOC pool size may be modified following woody encroachment (Boutton *et al.* 1998; Jackson *et al.* 2002; Chiti *et al.* 2017). This implies that potentially strong spatial gradients of SOC may exist along the soil profile at the landscape scale, because organic matter inputs from litterfall and root turnover will be more concentrated in topsoil compared to deeper portions of the profile. Given the fact that most studies on spatial patterns of SOC following woody encroachment have been conducted on surface soils, and that substantial SOC is stored in subsurface soils, this represents a major knowledge gap concerning the effects of vegetation cover change on the pattern of spatial heterogeneity in SOC along the soil profile.

The primary purpose of this study was to determine how woody encroachment into grassland affects the direction, magnitude and pattern of spatial heterogeneity in SOC along the soil profile. To accomplish this, spatially specific soil samples to a depth of 1·2 m were collected across a landscape in a subtropical savanna ecosystem, where woody plants have been encroaching into grasslands for the past century (Archer *et al.* 1988; Boutton *et al.* 1998). Our specific objectives were to: (i) estimate SOC stocks following woody encroachment and the proportion of these stocks derived from woody plants based on $\delta^{13}C$ values of SOC along the soil profile; (ii) quantify the pattern of spatial heterogeneity in SOC across this landscape and throughout the soil profile; and (iii) elucidate factors responsible for the variances in SOC across this landscape and throughout the soil profile. We hypothesized that woody encroachment into this grasslands would substantially: (i) increase SOC sequestrations to considerable depth, albeit at reduced magnitudes in deeper portions of the soil profile and (ii) alter the pattern of spatial heterogeneity in SOC along the soil profile.

Materials and methods

STUDY SITE

This study was conducted in the Rio Grande Plains region at the Texas A&M AgriLife La Copita Research Area (27°40′N, 98°12′W) in Jim Wells County, 65 km west of Corpus Christi, Texas, USA. The climate is subtropical, with a mean annual temperature of 22·4 °C and mean annual precipitation of 680 mm. Rainfall peaks occur in May and September. Elevation ranges from 75 to 90 m above sea level. Topography is relatively flat, with 1–3% slopes where uplands transition to low-lying portions of the landscape.

This study was confined to upland portions of the landscape where soils are primarily sandy loam Typic Argiustolls with a laterally continuous subsurface argillic horizon (*Bt*); however, some portions of the upland landscape have patches where the *Bt* horizon is absent (i.e. non-argillic inclusions), and these soils classify as Typic Haplustepts (Loomis 1989; Archer 1995; Zhou *et al.* 2017). The vegetation is characterized as subtropical savanna parkland, consisting of an herbaceous matrix comprised of C_4 grasses and C_3 forbs, with discrete woody patches interspersed throughout the herbaceous matrix. Woody patches are categorized into small shrub clusters and large groves. Clusters with diameters of <10 m are comprised of a single N-fixing *Prosopis glandulosa* tree with up to 15 understorey shrub/tree species. Groves with diameters of >10 m occur exclusively on non-argillic inclusions, and are comprised of several clusters that have fused together (Archer 1995; Bai *et al.* 2012; Zhou *et al.* 2017). Common understorey shrub/tree species in clusters and groves include *Zanthoxylum fagara*, *Schaefferia cuneifolia*, *Celtis pallida*, *Zizyphus obtusifolia*, *Lycium berlandieri*, *Mahonia trifoliolata* and *Opuntia leptocaulis*. In the herbaceous matrix, dominant C_4 grasses include *Paspalum setaceum*, *Setaria geniculata*, *Bouteloua rigidiseta* and *Chloris cucullata*, and dominant C_3 forbs include *Croton texensis*, *Wedelia texana*, *Ambrosia confertiflora* and *Parthenium hysterophorus*. Additional details on vegetation can be found in Archer *et al.* (1988) and Archer (1995).

FIELD SAMPLING

A 100 m × 160 m landscape divided into 10 m × 10 m grid cells was established on an upland portion of this study site in January 2002 (Bai *et al.* 2009; Liu *et al.* 2011) that included all three of the major upland landscape elements: grassland, cluster and grove (Fig. 1). The corners of each cell were georeferenced based on the UTM coordinates system (14 North, WGS 1984) using a GPS unit (Trimble Pathfinder Pro XRS; Trimble Navigation Limited, Sunnyvale, CA, USA). In July 2014, two randomly located points were selected within each 10 m × 10 m grid cell, yielding a total of 320 sample points within this 100 m × 160 m plot (Fig. 1). Landscape element types for each sample point were categorized as grassland, cluster or grove based on the size of canopy area. The distances from each sample point to two georeferenced cell corners were recorded. At each of the two sample points in each cell, two adjacent soil cores (28 mm in diameter ×120 cm in length) were collected using the PN150 JMC Environmentalist's Subsoil Probe (Clements Associates Inc., Newton, IA, USA). Each soil core was subdivided into six depth increments (0–5, 5–15, 15–30, 30–50, 50–80 and 80–120 cm). One soil core was oven-dried (105 °C for 48 h) to determine soil bulk density; the other core was air-dried prior to subsequent analyses. A colour-infrared aerial photograph (6 cm × 6 cm resolution) of this 100 m × 160 m landscape was acquired in July 2015, and used to compute the Normalized Difference Vegetation Index (NDVI = [NIR − RED]/[NIR + RED], in which NIR and RED represent the spectral reflectance measurements from the near-infrared and the red regions of the aerial photograph respectively).

LABORATORY ANALYSES

Soils used to determine bulk density were subsequently used to estimate fine (<2 mm) and coarse (>2 mm) root biomass by washing through sieves. No attempt was made to distinguish between live or dead roots. Roots were dried at 65 °C and weighed to determine root biomass. For elemental and isotopic analyses, three composite fine root samples were created for each landscape element by combining fine roots from 10 cores for each depth increment. Composite fine roots were homogenized and pulverized in a Mixer Mill MM 400 (Retsch GmbH, Haan, Germany).

Air-dried soil samples were passed through a 2-mm sieve to remove coarse organic fragments. No gravel was present in these soils. An aliquot of sieved soil was used to determine soil texture by the hydrometer method (Sheldrick & Wang 1993). Soil pH was determined on a 1:2 (soil: 0·01 mol L^{-1} $CaCl_2$) mixture using a glass electrode. An aliquot of sieved soil was dried at 60 °C for 48 h and pulverized in a centrifugal mill (Angstrom, Inc., Belleville, MI, USA). Pulverized soil samples were weighed into silver capsules (5 mm × 7 mm), treated with HCl vapour in a desiccator to remove carbonates for 8 h (Harris, Horwáth & van Kessel 2001), and then dried.

Carbon concentrations and the $\delta^{13}C$ values of acid-treated and dried soils and fine roots were determined using a Costech ECS 4010 elemental combustion system (Costech Analytical Technologies Inc., Valencia, CA, USA) interfaced via a ConFlo IV device with a Delta V Advantage isotope ratio mass spectrometer (Thermo Scientific, Bremen, Germany). Carbon isotope ratios are presented in δ notation (eqn 1):

$$\delta = \left(\frac{R_{\mathrm{sample}} - R_{\mathrm{STD}}}{R_{\mathrm{STD}}}\right) \times 10^3 \qquad \text{eqn 1}$$

where R_{Sample} is the $^{13}C/^{12}C$ ratio of the soil sample and R_{STD} is the $^{13}C/^{12}C$ ratio of the V-PDB standard. Precision of duplicate measurements was 0·1‰ for $\delta^{13}C$ for both soil and fine root samples.

DATA ANALYSES

Soil organic carbon stocks (Mg C ha^{-1}) were calculated based on the following equation:

$$\mathrm{Mg\ C\ ha^{-1}} = \left(\frac{C_c}{1000}\right) \times \mathrm{SBD} \times D \times 10^2 \qquad \text{eqn 2}$$

where C_c is SOC concentration (g C kg^{-1} soil), SBD is soil bulk density (g cm^{-3}) and D is the depth interval (or thickness) in cm for each depth increment. To facilitate comparisons between the unequal sampling depth intervals, we conducted our analyses on SOC density (kg C m^{-3}), amount of C per unit volume of soil, which was calculated using the following equation:

$$\mathrm{kg\ C\ m^{-3}} = \left(\frac{C_c}{1000}\right) \times \mathrm{SBD} \times 10^3 \qquad \text{eqn 3}$$

An identical soil sampling regime (i.e. two randomly located sampling points per 10 m × 10 m grid cell) was used to collect surface soils (0–15 cm) when this 100 m × 160 m landscape was established in 2002 (see Liu *et al.* 2011 for more details), and we used this previous dataset in conjunction with our new measurements to estimate SOC accumulation rates in surface soils for each landscape element during the past 12 years (2002–2014). To accomplish this, we combined our SOC stocks in the 0–5 and 5–15 cm depth increments obtained in 2014, and then compared them with stocks obtained in 2002.

Datasets that were not normally distributed were log-transformed before variable means of different landscape elements for each soil depth increment were compared using mixed models. Spatial autocorrelation of variables was taken into account as a spatial covariance for adjustment in mixed models (Littell *et al.* 2006). In mixed models, spherical, exponential and Gaussian structures were tested, and the best fitting model for each variable in each soil depth increment was selected based on Akaike information criterion (AIC). *Post hoc* comparisons of these variables in different landscape elements were also conducted using the mixed models with Tukey's correction. A

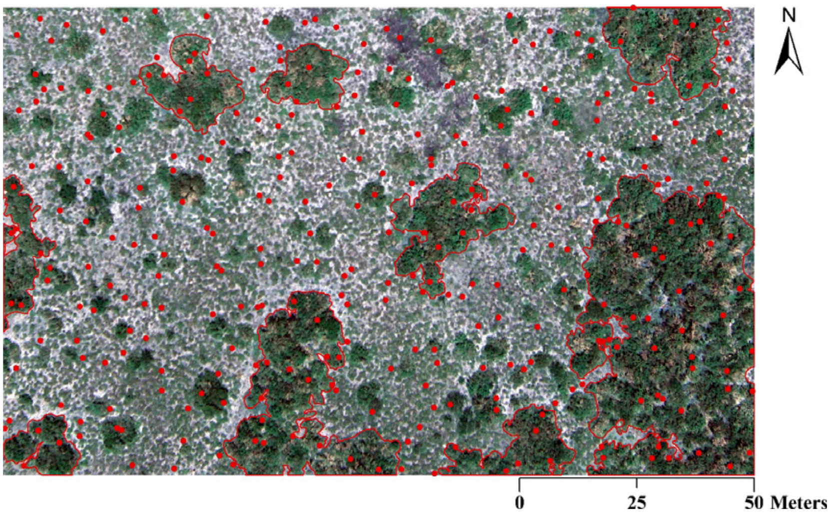

Fig. 1. Aerial photograph of the 100 m × 160 m study area and locations of 320 random soil samples (red points). Green patches are shrub clusters and groves (highlighted with red lines) and light grey colour indicates open grassland.

cut-off value of $P < 0{\cdot}05$ was used to indicate significant differences. Mixed models were performed using JMP pro 12.0 (SAS Institute Inc., Cary, NC, USA).

The relative proportions of SOC derived from woody plants (F) for each depth increment under woody patches (hereafter, clusters and groves) were calculated using a mass balance (eqn 4):

$$F = \frac{\delta_{WS} - \delta_{GS}}{\delta_{WR} - \delta_{GS}} \quad \text{eqn 4}$$

where δ_{WS} is the $\delta^{13}C$ value of SOC in woody patches for each depth increment; δ_{GS} is the average $\delta^{13}C$ value of SOC in remnant grassland soils (n = 200) for each depth increment; δ_{WR} is the average $\delta^{13}C$ value of fine roots in woody patches for each depth increments. Here, we assumed that (i) prior to woody encroachment, the $\delta^{13}C$ of SOC in grasslands was relatively homogeneous across this landscape and the average values for each depth increment were used as baselines; (ii) SOC derived from woody plants in wooded landscape elements had the same $\delta^{13}C$ values as those of fine roots in each depth increment as roots and root exudates are the main sources of C input into subsoil (Rumpel & Kögel-Knabner 2011), and even in topsoil, root-derived C is retained in soils much more efficiently than C derived from above-ground litterfall (Rasse, Rumpel & Dignac 2005; Schmidt *et al.* 2011; Clemmensen *et al.* 2013).

A sample variogram fitted with a variogram model was developed to quantify the spatial structure of SOC density based on values of 320 random sample points for each depth increment using R statistical software (R Development Core Team 2011, see Appendix S1, Supporting Information, Table S1, and Fig. S1 for more details). Ordinary kriging based on the best fitted variogram model was used to predict SOC densities at unsampled locations for each soil depth increment. Kriged maps of SOC density for each depth increment with a 0·5 m × 0·5 m resolution were generated in ArcMap 10.1 (ESRI, Redlands, CA, USA) using the Spatial Analyst tool.

Lacunarity was used to assess the spatial heterogeneity of SOC density for each depth increment across this landscape. Lacunarity is a scale-dependent measurement of spatial heterogeneity or the ‘gappiness’ of a landscape structure (Plotnick *et al.* 1996). Lacunarity was calculated based on each kriged map of SOC density. Briefly, a gliding box algorithm at eight different spatial scales with corresponding box sizes (side length of the gliding box, r) of 0·5, 1, 2, 4, 8, 16, 32 and 64 m was used to determine the lacunarity value of each kriged map. The gliding box of a given size (r) was first placed at one corner of the kriged map, and the ‘box mass’ S(r), the sum of SOC density of the pixels within the box, was determined. The box was then systematically moved through the map one pixel at a time and the box mass was recorded at each location. The lacunarity value $\Lambda(r)$ was calculated according to eqn 5:

$$\Lambda(r) = \frac{\mathrm{Var}(\mathrm{S}(r))}{\mathrm{E}(\mathrm{S}(r))^2} + 1 \quad \text{eqn 5}$$

where E(S(r)) is the mean and Var(S(r)) is the variance of the box mass S(r) for given box size r. All calculations were performed using R statistical software (R Development Core Team 2011). The lacunarity curve, natural log transformation of lacunarity values $\Lambda(r)$ against box size (r), was plotted to quantify the spatial heterogeneity of SOC density at different scales for each soil depth increment, with a higher value of lacunarity indicating a more heterogeneous distribution pattern across the landscape.

A spatial generalized least squares (GLS) model that incorporates spatial structure in the error term of the regression model (Beale *et al.* 2010) was used to analyse the relationships among the explanatory variables and SOC density within each soil depth increment and across this landscape. Explanatory variables included vegetation factors (NDVI and fine root biomass) and soil physical factors (soil bulk density, soil clay and silt contents, and soil pH). We excluded soil sand content as explanatory variable because of its high correlation with soil clay content. We initially explored the spatial autocorrelation in both the explanatory variables and response variable for each soil depth increment, then we tested different models with spatial structure (assuming linear, spherical, exponential and Gaussian structure) and non-spatial structure. The best fitting model for each soil depth increment was selected using the AIC. Parameters were estimated based on restricted maximum likelihood. The t-values for explanatory variables were used to indicate their relative importance in explanation of response variable (Diniz-Filho, Bini & Hawkins 2003). Analyses were performed using R statistical software (R Development Core Team 2011).

Results

VEGETATION AND SOIL CHARACTERISTICS

Overall, grasslands, clusters and groves covered 62·4%, 10·3% and 27·3% of this 100 m × 160 m landscape respectively (Table S2). Woody patches (both clusters and groves) exhibited significantly higher NDVI values than grasslands (Table S2). Soil bulk densities of woody patches were significantly lower than those of grasslands throughout the entire soil profile (Table 1). Due to the presence of non-argillic inclusions interspersed within a laterally continuous subsurface argillic horizon, and the fact that groves occurred only on these non-argillic inclusions (Zhou *et al.* 2017), groves had significantly lower clay content than grasslands in the 30–50, 50–80 and 80–120 cm depth increments (Table 1). Woody patches had higher pH values than grasslands throughout the entire soil profile (Table 1).

Woody patches had significantly higher root densities (kg m^{-3}) than grasslands throughout the entire soil profile (Fig. 2a,b). For example, in the 0–5 cm depth increment, average fine root densities of clusters ($10{\cdot}12 \pm 0{\cdot}69$ kg m^{-3}) and groves ($10{\cdot}20 \pm 0{\cdot}44$ kg m^{-3}) were almost three times higher than those of grasslands ($3{\cdot}47 \pm 0{\cdot}11$ kg m^{-3}). Fine and total root density decreased dramatically along the soil profile (Fig. 2a,b). However, the absolute magnitudes of root biomass stock (Mg ha^{-1}) in deeper soil increments were still remarkable (Fig. S2). For example, in the 80–120 cm depth increment, mean fine root biomass stocks of grasslands, clusters and groves were $1{\cdot}19 \pm 0{\cdot}05$, $2{\cdot}21 \pm 0{\cdot}16$ and $3{\cdot}07 \pm 0{\cdot}15$ Mg ha^{-1} respectively (Fig. S2).

SOC STORAGE AND $\delta^{13}C$ VALUES ALONG THE SOIL PROFILE

Woody patches had significantly higher SOC densities (kg C m^{-3}) than those of grasslands for all depth increments, except at 30–50 cm (Fig. 3a). Soil organic carbon densities decreased along the soil profile (Fig. 3a), while cumulative SOC stock (Mg C ha^{-1}) increased with depth (Table 2). Woody patches had higher SOC stocks than grasslands for each depth increment (Table 2). Overall, to a depth of 120 cm, cumulative SOC stocks for grasslands, clusters and groves were: $68{\cdot}30 \pm 0{\cdot}45$, $81{\cdot}17 \pm 1{\cdot}82$ and $86{\cdot}97 \pm 1{\cdot}40$ Mg C ha^{-1} respectively (Table 2). Soil organic carbon sequestration following woody encroachment was observed in the full 120 cm soil profile, albeit at reduced magnitudes in deeper portions of the profile; clusters and groves accumulated 12·87 and 18·67 Mg C ha^{-1} more SOC than grasslands respectively (Fig. 3b). Estimated SOC accumulation rates for groves and clusters in the 0–15 cm depth increment during the past 12 years (2002–2014) were 41·5 and 38·8 g C m^{-2} $year^{-1}$ respectively (Fig. 4).

Mean soil $\delta^{13}C$ values beneath grasslands range from −20·7‰ near the soil surface to −15·9‰ deeper in the profile (Table 3), reflecting the mixed C_4 grass/C_3 forb composition of the grassland. Mean soil $\delta^{13}C$ values beneath woody patches (−24·3 to −16·4‰) were significantly lower than those beneath grasslands throughout the entire soil profile, but higher than those of woody fine roots (−26·6 to −26·0‰) (Table 3), indicating current SOC beneath woody patches was comprised of both C derived from woody plants during the recent shift of vegetation cover as well as legacy C derived from the original grasslands that once dominated this region. Mass balance calculation revealed that 60·5% and 62·3% of soil C beneath clusters and groves were derived from woody plants in the 0–5 cm depth increment respectively (Table 3). The proportions of SOC derived from woody plants beneath woody patches decreased along the soil profile (Table 3); however, even in the 80–120 cm depth increment, 6·52% and 8·44% of SOC was derived from woody plants in clusters and groves respectively (Table 3).

PATTERN OF SPATIAL HETEROGENEITY IN SOC DENSITY ALONG THE SOIL PROFILE

Visual comparison of the kriged map of SOC density in the 0–5 cm depth increment (Fig. 4) with aerial photography of this landscape (Fig. 1) reveals a strong resemblance of the spatial pattern of SOC density to that of vegetation cover. Soil organic carbon densities were highest at the centres of woody patches, decreased towards the canopy edges of woody patches, and reached lowest values within the grassland matrix (Figs 1 and 5). However, this strong pattern became weaker in the 5–15 cm depth increment, and grew less distinct with increasing depth along the soil profile (Figs 1 and 5). In fact, SOC density in the 0–5 cm depth increment ranged from 5·35 to 73·90 kg C m^{-3}, and had a higher variability (coefficient of variation (CV) = 71·61%) than other depth increments (CVs range from 13·75% to 27·54%) (Table S3). Lacunarity analysis based on kriged maps also indicated that the 0–5 cm depth increment had significantly higher lacunarity values than other depth increments (Fig. 6), indicating that the 0–5 cm depth increment had a spatially more heterogeneous distribution of SOC density across this landscape.

Spatial GLS models revealed that vegetation factors (i.e. NDVI and fine root density), especially fine root density, were the most important explanatory variables for variation in SOC density in the 0–5 and 5–15 cm depth increments across this landscape (Table 4). However, from 15 to 120 cm in the soil profile, a combination of vegetation factors and soil physical factors, especially soil clay content, was responsible for the variation in SOC density across this landscape (Table 4).

Discussion

INCREASED SOC SEQUESTRATION THROUGHOUT THE PROFILE

Overall, our results indicate grassland-to-woodland conversion substantially increased SOC sequestration which is consistent with other studies in South America (e.g. González-Roglich *et al.* 2014), Australia (e.g. Daryanto, Eldridge & Throop 2013a), South Africa (e.g. Blaser *et al.* 2014; Chiti *et al.* 2017) and Europe (e.g. Maestre *et al.* 2009). More importantly, we observed that SOC sequestration following woody encroachment occurred at considerable soil depth, albeit to a lesser degree in deeper portions of the soil profile. Thus, these results support our first hypothesis.

Table 1. Mean and standard error (SE) of soil bulk density (g cm^{-3}), soil sand, silt and clay content (%), and soil pH in different landscape elements across this 100 m × 160 m landscape throughout the soil profile

Variables	Vegetation type	Soil depth (cm) 0–5	5–15	15–30	30–50	50–80	80–120
Soil bulk density	Grassland	1·34 ± 0·01^{a}	1·44 ± 0·00^{a}	1·41 ± 0·01^{a}	1·46 ± 0·00^{a}	1·52 ± 0·00^{a}	1·62 ± 0·00^{a}
	Cluster	1·10 ± 0·02^{b}	1·29 ± 0·01^{b}	1·36 ± 0·01^{b}	1·43 ± 0·01^{b}	1·49 ± 0·01^{b}	1·59 ± 0·01^{b}
	Grove	1·06 ± 0·01^{b}	1·31 ± 0·01^{b}	1·37 ± 0·01^{b}	1·43 ± 0·01^{b}	1·47 ± 0·01^{b}	1·59 ± 0·01^{b}
Soil sand content	Grassland	76·4 (0·2)^{a}	74·5 (0·2)^{a}	71·5 (0·1)^{a}	67·2 (0·2)^{b}	62·9 (0·2)^{b}	55·8 (0·3)^{b}
	Cluster	75·4 (0·4)^{a}	74·1 (0·4)^{ab}	71·4 (0·4)^{ab}	67·8 (0·6)^{ab}	63·0 (0·8)^{b}	55·4 (0·9)^{b}
	Grove	75·0 (0·4)^{b}	73·3 (0·4)^{b}	70·4 (0·5)^{b}	68·1 (0·5)^{a}	64·9 (0·6)^{a}	59·0 (0·9)^{a}
Soil silt content	Grassland	10·8 (0·1)^{b}	10·1 (0·1)^{a}	10·7 (0·1)^{a}	11·1 (0·1)^{a}	12·2 (0·1)^{a}	14·1 (0·1)^{a}
	Cluster	11·1 (0·2)^{a}	10·7 (0·2)^{a}	11·1 (0·2)^{a}	11·3 (0·2)^{a}	12·2 (0·2)^{a}	14·0 (0·2)^{a}
	Grove	11·8 (0·2)^{a}	11·2 (0·2)^{a}	11·7 (0·1)^{a}	11·9 (0·1)^{a}	12·2 (0·1)^{a}	13·5 (0·2)^{b}
Soil clay content	Grassland	12·8 ± 0·1^{a}	15·4 ± 0·1^{a}	17·8 ± 0·1^{a}	21·7 ± 0·2^{a}	25·0 ± 0·2^{a}	30·1 ± 0·3^{a}
	Cluster	13·5 ± 0·3^{a}	15·2 ± 0·3^{a}	17·5 ± 0·3^{a}	20·9 ± 0·6^{b}	24·9 ± 0·7^{a}	30·6 ± 0·7^{a}
	Grove	13·2 ± 0·3^{a}	15·5 ± 0·3^{a}	17·9 ± 0·3^{a}	20·0 ± 0·4^{c}	22·9 ± 0·5^{b}	27·6 ± 0·7^{b}
pH	Grassland	7·34 ± 0·02^{a}	7·21 ± 0·03^{b}	7·17 ± 0·03^{b}	7·30 ± 0·02^{b}	7·54 ± 0·02^{b}	7·74 ± 0·01^{b}
	Cluster	7·34 ± 0·04^{a}	7·34 ± 0·04^{a}	7·35 ± 0·06^{a}	7·46 ± 0·05^{a}	7·65 ± 0·03^{a}	7·79 ± 0·02^{a}
	Grove	7·39 ± 0·04^{a}	7·48 ± 0·03^{a}	7·54 ± 0·04^{a}	7·64 ± 0·04^{a}	7·74 ± 0·03^{a}	7·82 ± 0·01^{a}

Number of samples: grassland = 200, cluster = 41 and grove = 79. Significant differences ($P < 0·05$) between means for landscape elements are indicated with different superscript letters.

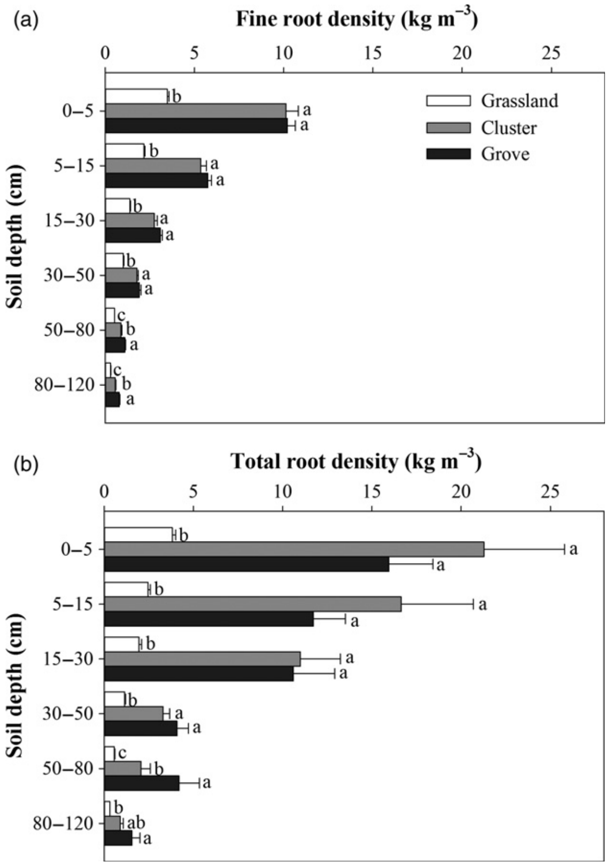

Fig. 2. Fine (a) and total root density (kg m^{-3}) (b) for different landscape elements across this 100 m × 160 m landscape throughout the soil profile. Significant differences ($P < 0·05$) between means for landscape elements are indicated with different letters. Number of samples: grassland = 200, cluster = 41 and grove = 79.

Although the 0–15 cm depth increment stored only around 20% of the cumulative SOC stock in the full 120 cm soil profile (Table 2), it accounted for more than half (57·75% and 59·23% for clusters and groves, respectively, Fig. 3b) of all the SOC sequestered following woody encroachment. Strong changes in topsoil C stock with increasing woody plant abundance have been observed in many grassland/savanna ecosystems around the world (see Barger *et al.* 2011; Eldridge *et al.* 2011; Blaser *et al.* 2014; Li *et al.* 2016 for reviews), with C accretion rates ranging from negative up to >100 g C m^{-2} year^{-1} depending on the encroaching species, stand age, land management practice, mean annual precipitation and soil sampling depth. Our estimated accumulation rates for both groves (41·5 g C m^{-2} year^{-1}) and clusters (38·8 g C m^{-2} year^{-1}) (Fig. 4) are higher than those estimated using a chronosequence approach spanning the past 120 years for this area (10–30 g C m^{-2} year^{-1} to 15 cm depth, Liao, Boutton & Jastrow 2006), but are within the range of values reported in reviews (Barger *et al.* 2011; Blaser *et al.* 2014). However, any attempts to account for relatively small temporal changes in SOC within such large soil volumes are subject to errors from amplified spatial variations in SOC in encroached ecosystems (Throop & Archer 2008; Liu *et al.* 2011) and climatic variations during the sampling time period.

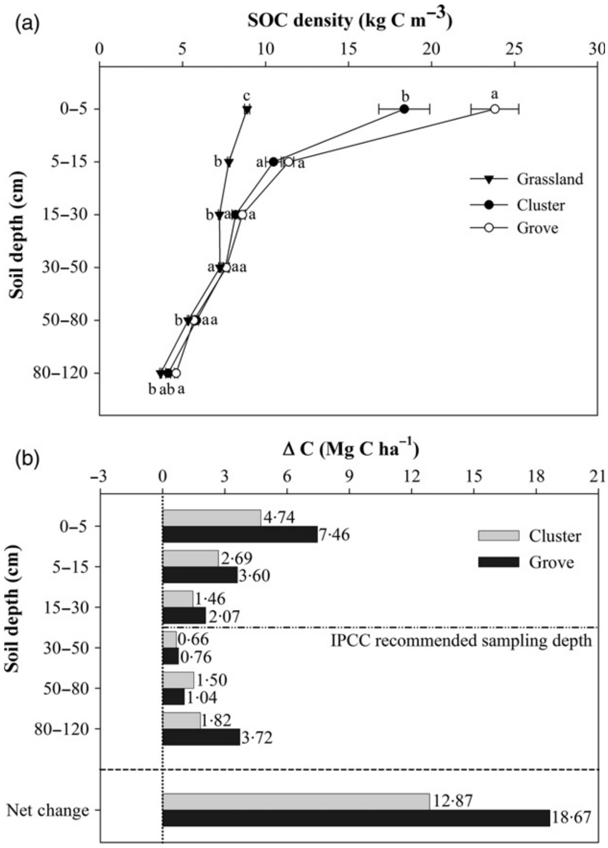

Fig. 3. Soil organic carbon (SOC) density (kg C m^{-3}) for different landscape elements along the soil profile (a) and averaged changes in SOC stock for clusters and groves compared to grasslands for each depth increment and in the full 0–120 cm profile (b) across this 100 m × 160 m landscape. Significant differences ($P < 0{\cdot}05$) between means for landscape elements are indicated with different letters. Number of samples: grassland = 200, cluster = 41 and grove = 79.

The results from this study also reveal that substantial SOC sequestration occurs in deeper portions of the soil profile following woody encroachment (Fig. 3b). Apart from dissolved organic C and soil faunal bioturbation, plant roots and root exudates are the primary sources of C input in subsoil (Jobbágy & Jackson 2000; Rumpel & Kögel-Knabner 2011). Plant growth forms differ in their rooting patterns, with trees/shrubs having root systems that are larger and deeper than grasses (Jackson *et al.* 1996; Schenk 2006). Thus, grassland-to-woodland conversions are expected to alter the depth and distribution of plant roots, and influence SOC stocks. In this study, we found significantly higher fine and total root densities beneath woody patches than beneath grasslands throughout the entire soil profile (Fig. 2). Even in the 80–120 cm depth increment, mean fine root densities of woody patches were still more than two times higher than those of grasslands (Fig. 2a). Considering the relatively rapid turnover rate of fine roots (Gill & Jackson 2000), this implies strong potential for the formation of SOC in subsoil. Lower δ^{13}C values of SOC in woody patches compared to grasslands confirm that C_3 woody plant roots are indeed contributing to SOC stocks, even at considerable soil depth (Table 3). However, SOC accumulation is regulated by processes influencing the balance between C inputs and losses (Six *et al.* 2002; Schmidt *et al.* 2011). In a long-term study of reforestation, subsoil losses of soil C were reported due to enhanced microbial activity and soil organic matter decomposition following vegetation cover change (Mobley *et al.* 2015). Thus, the future trajectory of SOC sequestration observed following woody encroachment in deeper portions of the soil profile remains an open question. Will the amount of SOC sequestered in subsoil be counterbalanced by the enhanced microbial decomposition (i.e. priming) following labile C input from woody plant roots (e.g. Fontaine *et al.* 2007)? Or, will the subsoil continue to accumulate C that is derived from deep roots as organic matter protection mechanisms in the subsoil may not yet be saturated?

AMPLIFIED PATTERN OF SPATIAL HETEROGENEITY IN SOC IN SURFACE SOIL

Several studies have quantified spatial heterogeneity of soil properties after woody encroachment (e.g. Throop & Archer 2008; Bai *et al.* 2009; Liu *et al.* 2011; Daryanto, Eldridge & Wang 2013b); however, none has explored the extent to which woody encroachment modifies the pattern of spatial heterogeneity in SOC in deeper soil layers. Our analyses revealed that woody encroachment significantly amplified the pattern of spatial heterogeneity in SOC in the 0–5 cm depth increment, had a smaller impact on 5–15 cm depth increment, but had no distinct influence on soils below 15 cm across this landscape. These minimal impacts at depths >15 cm cause us to reject our second hypothesis that woody encroachment would substantially alter the pattern of spatial heterogeneity in SOC throughout the soil profile.

The spatial patterns of SOC in the 0–5 cm depth increment indicated that SOC values were highest near the centres of woody patches, decreased towards the canopy edges, and reached lowest values in grasslands (Fig. 5). Previous studies show that SOC accumulation is initiated once woody patches/plants establish in grasslands (Schlesinger *et al.* 1996; Maestre *et al.* 2009; Daryanto, Eldridge & Throop 2013a), and that this SOC accumulation is positively correlated with the size or age of woody patches/plants (Liao, Boutton & Jastrow 2006; McClaran *et al.* 2008; Blaser *et al.* 2014). Therefore, our observed SOC spatial gradient from the centre to edge of the woody patches likely reflects the size and/or age of the woody patch, and the rate at which it expands laterally into the grassland (Throop & Archer 2008; Bai *et al.* 2012). Based on historical accounts, tree rings and soil δ^{13}C analyses, it is well-established that the conversion of grasslands to the current landscape began in the mid to late 1800s in this area (Archer 1995; Boutton *et al.* 1998; Bai *et al.* 2009). Because the woody vegetation near the centres of clusters and groves is older (>100 years) than near the periphery of those woody patches (Bai *et al.* 2012), there has been more time for SOC to accumulate near the central portions of these woody patches compared to their peripheral areas near the boundary with grassland. Consequently, the strong SOC gradients within woody patches

Soil depth (cm)	Grassland	Cluster	Grove
(a) SOC stock (Mg C ha^{-1})			
0–5	4·44 ± 0·08[c]	9·18 ± 0·77[b]	11·91 ± 0·72[a]
5–15	7·79 ± 0·07[b]	10·48 ± 0·47[a]	11·39 ± 0·30[a]
15–30	10·83 ± 0·10[b]	12·29 ± 0·32[a]	12·90 ± 0·25[a]
30–50	14·50 ± 0·14[a]	15·16 ± 0·30[a]	15·27 ± 0·36[a]
50–80	16·00 ± 0·13[b]	17·51 ± 0·39[a]	17·05 ± 0·30[a]
80–120	14·73 ± 0·20[c]	16·55 ± 0·59[b]	18·45 ± 0·38[a]
(b) Cumulative SOC stock (Mg C ha^{-1})			
Surface to 5 cm	4·44 ± 0·08[c] (6·5)	9·18 ± 0·77[b] (11·0)	11·91 ± 0·72[a] (13·3)
Surface to 15 cm	12·23 ± 0·13[c] (17. 9)	19·66 ± 1·16[b] (23·8)	23·30 ± 0·91[a] (26·4)
Surface to 30 cm	**23·07 ± 0·19[c] (33. 8)**	**31·95 ± 1·37[b] (39·0)**	**36·21 ± 1·01[a] (41·3)**
Surface to 50 cm	37·57 ± 0·27[c] (55·1)	47·12 ± 1·51[b] (58·0)	51·48 ± 1·13[a] (58·9)
Surface to 80 cm	53·58 ± 0·36[c] (78·5)	64·62 ± 1·63[b] (79·6)	68·52 ± 1·21[a] (78·7)
Surface to 120 cm	68·30 ± 0·45[c] (100·0)	81·17 ± 1·92[b] (100·0)	86·97 ± 1·40[a] (100·0)

Table 2. Mean and standard error (SE) of soil organic carbon (SOC) stock (Mg C ha^{-1}) (a) and cumulative SOC stock (Mg C ha^{-1}) (b) for different landscape elements across this 100 m × 160 m landscape throughout the soil profile

Numbers in the parentheses are percentages of cumulative SOC stock from the surface to the specified depth divided by the cumulative SOC stock to a depth of 120 cm. Row with text in bold indicates the IPCC recommended sampling depth (30 cm). Number of samples: grassland = 200, cluster = 41 and grove = 79. Significant differences ($P < 0{\cdot}05$) between means for landscape elements are indicated with different superscript letters.

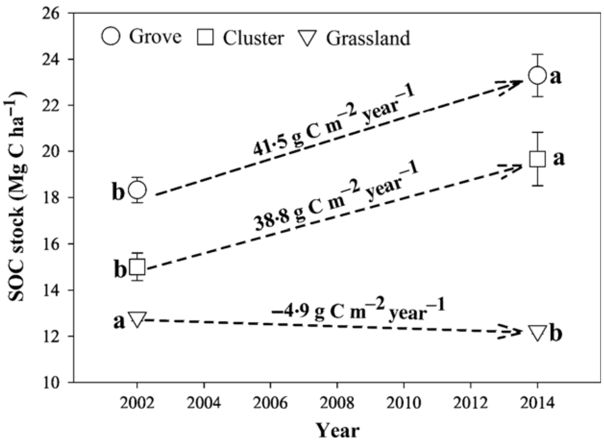

Fig. 4. Soil organic carbon (SOC) accumulation rates at the 0–15 cm depth increment for different landscape elements from 2002 to 2014 for this 100 m × 160 m landscape. SOC stocks (Mg C ha^{-1}) for 2002 were reported in Liu *et al.* 2011. Significant differences ($P < 0{\cdot}05$) between means for landscape elements are indicated with different letters based on unpaired *t*-test.

coupled with dramatic differences in SOC between woody patches and open grasslands creates strong pattern of spatial heterogeneity across this landscape (Fig. 6).

Contrary to our hypothesis, we did not observe substantial impacts of woody encroachment on the pattern of spatial heterogeneity in SOC below the 15 cm depth. However, we did find root density, the primary sources of C inputs into subsoil (Rumpel & Kögel-Knabner 2011), was significantly higher under woody patches than under grasslands (Fig. 2); and spatial patterns of root distribution for each depth increment strongly resembled vegetation patterns (unpublished data). In addition, the spatial patterns of soil $\delta^{13}C$ also strongly resembled vegetation pattern throughout the soil profile (unpublished data). This raises the issue of why spatial patterns of roots and soil $\delta^{13}C$ values resembled those of vegetation cover (even below 15 cm depth), while those of SOC did not. There are two possible explanations for this discrepancy.

Firstly, results from this study are a response to woody patches that are relatively young (c. 100 years, Archer 1995; Bai *et al.* 2009) from a SOC stabilization perspective. Dynamic simulation models indicate that it may take c. 200 years to reach plant C stabilization after woody encroachment, with SOC stabilization in the topsoil (0–20 cm) not occurring until c. 400 after woody encroachment in this area (Hibbard *et al.* 2003). As C input declines with soil depth, subsoil (below 20 cm) may need more time to reach SOC stabilization/saturation. Therefore, we predict that, without any disturbances (i.e. fire, brush management), woody encroachment into this landscape will continue to alter the spatial heterogeneity of SOC in subsoil for at least the next 400 years.

Secondly, many mechanisms have been identified to account for the accumulation/stabilization of organic matter in soils (Six *et al.* 2002; Rumpel & Kögel-Knabner 2011; Schmidt *et al.* 2011), and C dynamics in topsoil and in subsoil may be controlled by different mechanisms (Salomé *et al.* 2010). In this study, we suggest that both biological and soil physical mechanisms contribute to the reduced influence of woody encroachment on spatial patterns and heterogeneity of SOC in deeper soil layers. This suggestion is supported by spatial GLS models which revealed that a combination of fine root density and soil clay content predicted more of the variability of SOC in soils below 15 cm depth (Table 4). These results suggest that physical protection, the intimate association of organic matter with soil minerals (i.e. clay particles) (Six *et al.* 2002), may have played an important role in SOC stabilization in subsoil across this landscape. Subsurface soils across this landscape are characterized by an argillic horizon

Table 3. Mean and standard error (SE) of $\delta^{13}C$ values (‰ vs. V-PDB) of soil organic carbon (SOC) and fine roots, and percentage (%) of SOC derived from woody plants in clusters and groves across this 100 m × 160 m landscape throughout the soil profile

	SOC $\delta^{13}C$ (‰)*			Fine root $\delta^{13}C$ (‰)†		Estimates (%) of SOC derived from woody plants‡	
Soil depths (cm)	Grassland	Cluster	Grove	Cluster	Grove	Cluster	Grove
0–5	$-20{\cdot}7 \pm 0{\cdot}1^{a}$	$-24{\cdot}3 \pm 0{\cdot}2^{b}$	$-24{\cdot}0 \pm 0{\cdot}2^{b}$	$-26{\cdot}6 \pm 0{\cdot}1$	$-26{\cdot}0 \pm 0{\cdot}2$	$60{\cdot}5 \pm 3{\cdot}6^{a}$	$62{\cdot}3 \pm 3{\cdot}1^{a}$
5–15	$-18{\cdot}3 \pm 0{\cdot}1^{a}$	$-21{\cdot}5 \pm 0{\cdot}2^{b}$	$-21{\cdot}4 \pm 0{\cdot}2^{b}$	$-26{\cdot}8 \pm 0{\cdot}2$	$-26{\cdot}4 \pm 0{\cdot}3$	$37{\cdot}6 \pm 2{\cdot}8^{a}$	$38{\cdot}9 \pm 2{\cdot}0^{a}$
15–30	$-16{\cdot}4 \pm 0{\cdot}1^{a}$	$-17{\cdot}6 \pm 0{\cdot}2^{b}$	$-18{\cdot}3 \pm 0{\cdot}2^{c}$	$-26{\cdot}3 \pm 0{\cdot}2$	$-26{\cdot}2 \pm 0{\cdot}2$	$15{\cdot}4 \pm 2{\cdot}2^{b}$	$21{\cdot}8 \pm 1{\cdot}7^{a}$
30–50	$-15{\cdot}9 \pm 0{\cdot}1^{a}$	$-16{\cdot}4 \pm 0{\cdot}2^{b}$	$-17{\cdot}3 \pm 0{\cdot}2^{c}$	$-26{\cdot}5 \pm 0{\cdot}2$	$-26{\cdot}1 \pm 0{\cdot}1$	$8{\cdot}0 \pm 1{\cdot}4^{b}$	$17{\cdot}4 \pm 1{\cdot}7^{a}$
50–80	$-15.\ 9 \pm 0{\cdot}1^{a}$	$-16{\cdot}7 \pm 0{\cdot}1^{b}$	$-17{\cdot}0 \pm 0{\cdot}1^{b}$	$-26{\cdot}4 \pm 0{\cdot}2$	$-26{\cdot}4 \pm 0{\cdot}1$	$7{\cdot}2 \pm 1{\cdot}1^{a}$	$10{\cdot}2 \pm 1{\cdot}2^{a}$
80–120	$-17{\cdot}0 \pm 0{\cdot}1^{a}$	$-17{\cdot}6 \pm 0{\cdot}1^{b}$	$-17{\cdot}8 \pm 0{\cdot}1^{b}$	$-26{\cdot}4 \pm 0{\cdot}3$	$-26{\cdot}3 \pm 0{\cdot}2$	$6{\cdot}5 \pm 1{\cdot}5^{a}$	$8{\cdot}4 \pm 1{\cdot}3^{a}$

*Number of samples: grassland = 200, cluster = 41 and grove = 79.
†Number of replicates: cluster = 3 and grove = 3.
‡Significance was based on unpaired *t*-test.
Significant differences ($P < 0{\cdot}05$) between means for landscape elements are indicated with different superscript letters.

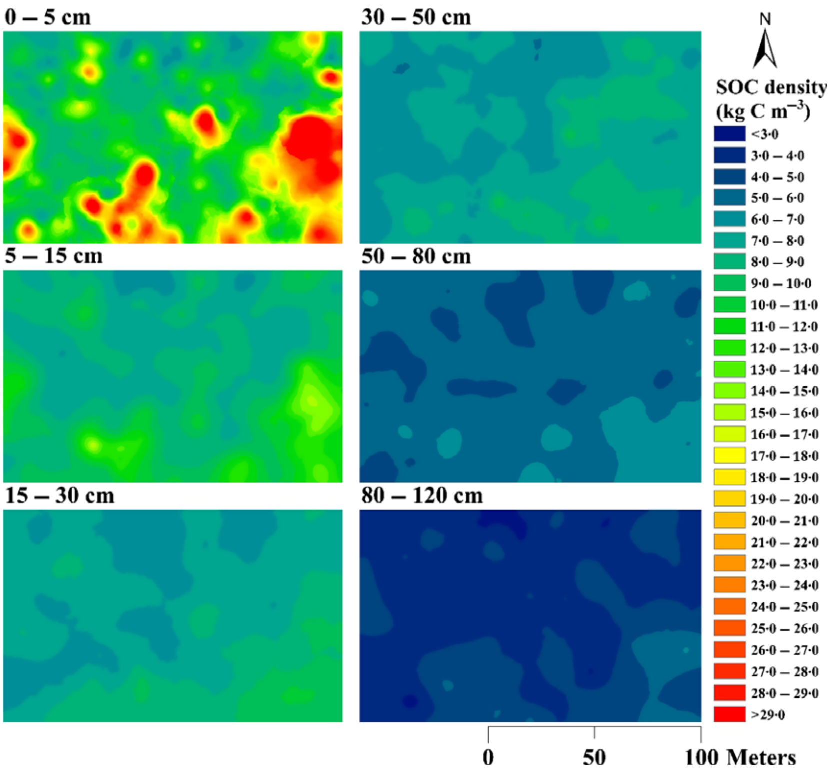

Fig. 5. Kriged maps of soil organic carbon (SOC) density (kg C m^{-3}) based on 320 randomly located sampling points for this 100 m × 160 m landscape throughout the soil profile.

which begins at c. 30 cm (Loomis 1989). However, non-argillic inclusions with coarse-textured subsoils are also present across this landscape and are usually covered by woody groves (Archer 1995; Zhou *et al.* 2017). Thus, higher C inputs from roots beneath groves may be offset by reduced physical protection due to coarse-textured subsoils. In contrast, lower C inputs under grasslands may be more effectively protected from decay by physical protection in the clayey argillic horizon. The net outcome is a great similarity in SOC density between woody patches and grasslands in deeper soil layers. This inference is supported by our results which showed no significant difference in SOC density between woody patches and grasslands (Fig. 3a), and reduced SOC accumulation (Table 2, Fig. 3b) in the 30–50 cm depth increment. These smaller discrepancies in SOC between woody patches and grasslands in deep portions of the profile may reduce spatial heterogeneity at deeper soil depths.

IMPLICATIONS FOR SOC ESTIMATES FOLLOWING VEGETATION COVER CHANGE

Our findings emphasize the importance of deep soil sampling to assess SOC inventories following woody encroachment, as highlighted in other land cover change studies (Don, Schumacher & Freibauer 2011; Mobley *et al.* 2015). For example, our results showed that c. 60% of the total

SOC stock to 120 cm depth across this landscape was found in soils below 30 cm depth (the IPCC recommended sampling depth) (Table 2). This is consistent with global estimates which show a 50–50 split in SOC stocks between 0–30 cm and 30–100 cm depth (Batjes 1996; Jobbágy & Jackson 2000). More important, in terms of SOC sequestration, 30% of total sequestered SOC to 120 cm depth across this landscape was stored below 30 cm depth following woody encroachment (Fig. 3b). This implies that current terrestrial C budgets likely underestimate the potential magnitude of C sequestration following woody encroachment due to the overlooked subsoil. Given the geographic extent of woody encroachment into grass-dominated ecosystems around the world (Eldridge *et al.* 2011; Stevens *et al.* 2017), taking deep SOC into account is critical to evaluate dryland ecosystem services in terms of climate change mitigation through C sequestration (Pacala *et al.* 2001; King *et al.* 2007; Dean *et al.* 2015). This recommendation of deep sampling to improve accurate soil C inventories also applies to studies of soil C dynamics following vegetation cover change in other ecosystem types. As SOC accumulation/stabilization in topsoil and subsoil is controlled by different regulatory mechanism according to this and other studies (Salomé *et al.* 2010; Rumpel & Kögel-Knabner 2011; Mobley *et al.* 2015), a better understanding of these mechanisms is essential to predict the vulnerability of deep SOC to vegetation cover change. Meanwhile, the amplified pattern of spatial heterogeneity in SOC density in the 0–5 cm depth increment following woody encroachment emphasizes that the majority of soil C studies working on surface soils should consider appropriate sample distribution and intensity to account for spatial heterogeneity and uncertainty of SOC in landscapes where complex vegetation cover exist. Limited sample sizes or inappropriate sample regimes that fail to capture the spatial gradient from centre to canopy edge of patchy vegetation (Throop & Archer 2008; Liu *et al.* 2011)

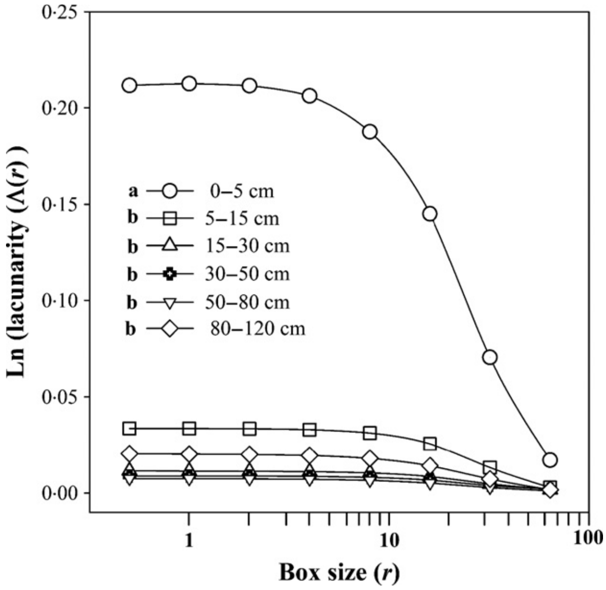

Fig. 6. Lacunarity curves along the soil profile derived from kriged maps of soil organic carbon (SOC) density. Significant differences ($P < 0{\cdot}05$) between different soil depth increments were detected based on one-way ANOVA (Student's *t*-test) and indicated with different letters.

Table 4. Best-fit regressions for soil organic carbon (SOC) density (kg C m^{-3}) as the response variable explained by explanatory variables according to spatial generalized least squares (GLS) models. Explanatory variables are vegetation variables including normalized difference vegetation index (NDVI), fine root density (kg m^{-3}) (FRD) and soil physical variables including soil bulk density (g cm^{-3}) (SBD), soil clay (%) and silt (%) contents and soil pH

		Vegetation variables		Soil physical variables				
Depth (cm)	Parameters	NDVI	FRD	SBD	Clay	Silt	pH	Intercept
0–5	Coefficients	**8·03**	**1·28**	−0·38	−0·22	0·70	−1·48	10·48
	t	**2·48**	**10·06**	−0·11	−0·80	1·80	−1·06	0·84
	P	**0·01**	**<0·0001**	0·91	0·42	0·07	0·29	0·40
5–15	Coefficients	**2·16**	**0·57**	−2·04	0·09	0·20	**0·66**	1·06
	t	**2·65**	**9·22**	−1·69	1·50	1·74	**2·11**	0·33
	P	**0·008**	**<0·0001**	0·09	0·13	0·08	**0·03**	0·74
15–30	Coefficients	**1·29**	**0·57**	**4·28**	**0·17**	0·13	**0·35**	**−6·85**
	t	**2·94**	**9·78**	**5·45**	**5·70**	1·84	**2·10**	**−3·90**
	P	**0·004**	**<0·0001**	**<0·0001**	**<0·0001**	0·07	**0·04**	**0·0001**
30–50	Coefficients	**1·71**	**0·50**	**5·15**	**0·19**	**0·26**	**−0·34**	**−5·71**
	t	**3·96**	**5·64**	**5·63**	**10·38**	**4·54**	**−1·90**	**−2·74**
	P	**0·0001**	**<0·0001**	**<0·0001**	**<0·0001**	**<0·0001**	**<0·0001**	**0·007**
50–80	Coefficients	0·54	**0·25**	0·91	**0·06**	**0·12**	0·02	0·73
	t	1·86	**2·18**	1·41	**4·15**	**2·82**	0·11	0·40
	P	0·06	**0·03**	0·16	**<0·0001**	**0·01**	0·91	0·69
80–120	Coefficients	0·56	**0·46**	−0·90	**0·03**	0·04	**1·41**	−7·32
	t	1·89	**3·10**	−0·98	**2·24**	0·89	**3·55**	−1·94
	P	0·06	**0·002**	0·33	**0·03**	0·38	**0·0004**	0·05

Bold text indicates significant variables ($P < 0{\cdot}05$).

may subsequently overestimate or underestimate the impact of vegetation cover change on SOC stocks and dynamics.

Conclusions

We found that woody encroachment into this landscape increased SOC storage throughout the upper 1·2 m of the soil profile, and 30% of the C sequestered following encroachment was stored below 30 cm. This highlights the merit and necessity of deep soil sampling to quantify SOC stocks and dynamics, which are not accounted for in the majority of soil C inventories following land cover/land use change (Don, Schumacher & Freibauer 2011). In addition, we found that woody encroachment into this landscape significantly altered the pattern of spatial heterogeneity in SOC in topsoil. However, spatial heterogeneity in subsoil SOC was less distinct and not related to vegetation distribution, perhaps due to variation in subsoil texture across the landscape, and/or inadequate time for deep soil C pools to respond to the relatively recent (c. 100 years) woody plant encroachment. Given the global extent of land cover change, these findings have important implications for current terrestrial C inventories/models and future management of SOC stock to mitigate climate change.

Author's contributions

Y.Z., T.W.B. and X.B.W. formulated the original idea and developed methodology; Y.Z. performed sample processing and statistical analysis; Y.Z., T.W.B. and X.B.W. interpreted the data; Y.Z. and T.W.B. wrote the manuscript with editorial advice from X.B.W. All authors contributed critically to the drafts and gave final approval for publication.

Acknowledgements

This research was supported by a Doctoral Dissertation Improvement Grant from the U.S. National Science Foundation (DEB/DDIG1600790), USDA/NIFA Hatch Project (1003961), an Exploration Fund Grant from the Explorers Club, and the Howard McCarley Student Research Award from the Southwestern Association of Naturalists. Y.Z. is supported by a Sid Kyle Graduate Merit Assistantship from the Department of Ecosystem Science and Management, Texas A&M University. We thank Dr. Ayumi Hyodo for technical support in the Stable Isotopes for Biosphere Sciences Lab at Texas A&M University, David and Stacy McKown for on-site logistics at the La Copita Research Area. We also thank two anonymous reviewers for improving the manuscript.

Data accessibility

Data available from the Dryad Digital Repository https://doi.org/10.5061/dryad.ns92q (Zhou, Boutton & Wu 2017).

References

Archer, S. (1995) Tree-grass dynamics in a *Prosopis*-thornscrub savanna parkland: reconstructing the past and predicting the future. *Ecoscience*, **2**, 83–99.

Archer, S., Scifres, C., Bassham, C.R. & Maggio, R. (1988) Autogenic succession in a subtropical savanna: conversion of grassland to thorn woodland. *Ecological Monographs*, **58**, 111–127.

Bai, E., Boutton, T.W., Wu, X.B., Liu, F. & Archer, S.R. (2009) Landscape-scale vegetation dynamics inferred from spatial patterns of soil δ^{13}C in a subtropical savanna parkland. *Journal of Geophysical Research: Biogeosciences*, **114**, G01019.

Bai, E., Boutton, T.W., Liu, F., Wu, X.B. & Archer, S.R. (2012) Spatial patterns of soil δ^{13}C reveal grassland-to-woodland successional processes. *Organic Geochemistry*, **42**, 1512–1518.

Bailey, R.G. (1996) *Ecosystem Geography*. Springer, New York, NY, USA.

Barger, N.N., Archer, S.R., Campbell, J.L., Huang, C., Morton, J.A. & Knapp, A.K. (2011) Woody plant proliferation in North American drylands: a synthesis of impacts on ecosystem carbon balance. *Journal of Geophysical Research: Biogeosciences*, **116**, G00K07.

Batjes, N.H. (1996) Total carbon and nitrogen in the soils of the world. *European Journal of Soil Science*, **47**, 151–163.

Beale, C.M., Lennon, J.J., Yearsley, J.M., Brewer, M.J. & Elston, D.A. (2010) Regression analysis of spatial data. *Ecology Letters*, **13**, 246–264.

Blaser, W.J., Shanungu, G.K., Edwards, P.J. & Olde Venterink, H. (2014) Woody encroachment reduces nutrient limitation and promotes soil carbon sequestration. *Ecology and Evolution*, **4**, 1423–1438.

Boutton, T.W., Archer, S.R. & Midwood, A.J. (1999) Stable isotopes in ecosystem science: structure, function and dynamics of a subtropical savanna. *Rapid Communications in Mass Spectrometry*, **13**, 1263–1277.

Boutton, T.W., Archer, S.R., Midwood, A.J., Zitzer, S.F. & Bol, R. (1998) δ^{13}C values of soil organic carbon and their use in documenting vegetation change in a subtropical savanna ecosystem. *Geoderma*, **82**, 5–41.

Chiti, T., Mihindou, V., Jeffery, K.J., Malhi, Y., De Oliveira, F.L., White, L.J. & Valentini, R. (2017) Impact of woody encroachment on soil organic carbon storage in the Lopé National Park, Gabon. *Biotropica*, **49**, 9–13.

Clemmensen, K.E., Bahr, A., Ovaskainen, O. *et al.* (2013) Roots and associated fungi drive long-term carbon sequestration in boreal forest. *Science*, **339**, 1615–1618.

Dalle, G., Maass, B.L. & Isselstein, J. (2006) Encroachment of woody plants and its impact on pastoral livestock production in the Borana lowlands, southern Oromia, Ethiopia. *African Journal of Ecology*, **44**, 237–246.

Daryanto, S., Eldridge, D.J. & Throop, H.L. (2013a) Managing semi-arid woodlands for carbon storage: grazing and shrub effects on above-and belowground carbon. *Agriculture, Ecosystems & Environment*, **169**, 1–11.

Daryanto, S., Eldridge, D.J. & Wang, L. (2013b) Ploughing and grazing alter the spatial patterning of surface soils in a shrub-encroached woodland. *Geoderma*, **200**, 67–76.

Dean, C., Kirkpatrick, J.B., Harper, R.J. & Eldridge, D.J. (2015) Optimising carbon sequestration in arid and semiarid rangelands. *Ecological Engineering*, **74**, 148–163.

Diniz-Filho, J.A.F., Bini, L.M. & Hawkins, B.A. (2003) Spatial autocorrelation and red herrings in geographical ecology. *Global Ecology and Biogeography*, **12**, 53–64.

Don, A., Schumacher, J. & Freibauer, A. (2011) Impact of tropical land-use change on soil organic carbon stocks–a meta-analysis. *Global Change Biology*, **17**, 1658–1670.

Eldridge, D.J., Bowker, M.A., Maestre, F., Roger, E., Reynolds, J. & Whitford, W.G. (2011) Impacts of shrub encroachment on ecosystem structure and functioning: towards a global synthesis. *Ecology Letters*, **14**, 709–722.

Fontaine, S., Barot, S., Barré, P., Bdioui, N., Mary, B. & Rumpel, C. (2007) Stability of organic carbon in deep soil layers controlled by fresh carbon supply. *Nature*, **450**, 277–280.

Gill, R.A. & Jackson, R.B. (2000) Global patterns of root turnover for terrestrial ecosystems. *New Phytologist*, **147**, 13–31.

González-Roglich, M., Swenson, J.J., Jobbágy, E.G. & Jackson, R.B. (2014) Shifting carbon pools along a plant cover gradient in woody encroached savannas of central Argentina. *Forest Ecology and Management*, **331**, 71–78.

Guo, L.B. & Gifford, R.M. (2002) Soil carbon stocks and land use change: a meta analysis. *Global Change Biology*, **8**, 345–360.

Harris, D., Horwáth, W.R. & van Kessel, C. (2001) Acid fumigation of soils to remove carbonates prior to total organic carbon or carbon-13 isotopic analysis. *Soil Science Society of America Journal*, **65**, 1853–1856.

Hibbard, K.A., Schimel, D.S., Archer, S., Ojima, D.S. & Parton, W. (2003) Grassland to woodland transitions: integrating changes in landscape structure and biogeochemistry. *Ecological Applications*, **13**, 911–926.

Hughes, R.F., Archer, S.R., Asner, G.P., Wessman, C.A., McMurtry, C., Nelson, J. & Ansley, R.J. (2006) Changes in aboveground primary production and carbon and nitrogen pools accompanying woody plant encroachment in a temperate savanna. *Global Change Biology*, **12**, 1733–1747.

Huxman, T.E., Wilcox, B.P., Breshears, D.D., Scott, R.L., Snyder, K.A., Small, E.E., Hultine, K., Pockman, W.T. & Jackson, R.B. (2005) Ecohydrological implications of woody plant encroachment. *Ecology*, **86**, 308–319.

IPCC (2006) Generic methodologies applicable to multiple land-use categories. *2006 IPCC Guidelines for National Greenhouse Gas Inventories. Volume 4. Agriculture, Forestry and Other Land Use* (eds H.S. Eggleston, L. Buendia, K. Miwa, T. Ngara & K. Tanabe), pp. 2.1–2.59. IGES, Hayama, Japan.

Jackson, R.B., Canadell, J., Ehleringer, J.R., Mooney, H.A., Sala, O.E. & Schulze, E.D. (1996) A global analysis of root distributions for terrestrial biomes. *Oecologia*, **108**, 389–411.

Jackson, R.B., Banner, J.L., Jobbagy, E.G., Pockman, W.T. & Wall, D.H. (2002) Ecosystem carbon loss with woody plant invasion of grasslands. *Nature*, **418**, 23–626.

Jobbágy, E.G. & Jackson, R.B. (2000) The vertical distribution of soil organic carbon and its relation to climate and vegetation. *Ecological Applications*, **10**, 423–436.

King, A.W., Dilling, L., Zimmerman, G.P., Fairman, D.M., Houghton, R.A., Marland, G., Rose, A.Z. & Wilbanks, T.J. (2007) Executive summary. *The First State of the Carbon Cycle Report (SOCCR): The North American Carbon Budget and Implications for the Global Carbon Cycle. A Report by the U.S. Climate Change Science Program and the Subcommittee on Global Change Research* (eds A.W. King, L. Dilling, G.P. Zimmerman, D.M. Fairman, R.A. Houghton, G. Marland, A.Z. Rose & T.J. Wilbanks), pp. 1–14. National Oceanic and Atmospheric Administration, National Climatic Data Center, Asheville, NC, USA.

Li, H., Shen, H., Chen, L. Liu, T., Hu, H., Zhao, X., Zhou, L., Zhang, P. & Fang, J. (2016) Effects of shrub encroachment on soil organic carbon in global grasslands. *Scientific Reports*, **6**, 28974. doi:10.1038/srep28974

Liao, J.D., Boutton, T.W. & Jastrow, J.D. (2006) Storage and dynamics of carbon and nitrogen in soil physical fractions following woody plant invasion of grassland. *Soil Biology and Biochemistry*, **38**, 3184–3196.

Littell, R.C., Milliken, G.A., Stroup, W.W., Wolfinger, R.D. & Schabenberger, O. (2006) *SAS for Mixed Models*. SAS Institute Inc., Cary, NC, USA.

Liu, F., Wu, X.B., Bai, E., Boutton, T.W. & Archer, S.R. (2011) Quantifying soil organic carbon in complex landscapes: an example of grassland undergoing encroachment of woody plants. *Global Change Biology*, **17**, 1119–1129.

Loomis, L.E. (1989) *Influence of heterogeneous subsoil development on vegetation patterns in a subtropical savanna parkland, Texas.* PhD Dissertation, Texas A&M University, College Station, TX, USA.

Maestre, F.T., Bowker, M.A., Puche, M.D. *et al.* (2009) Shrub encroachment can reverse desertification in semi-arid Mediterranean grasslands. *Ecology Letters*, **12**, 930–941.

McClaran, M.P., Moore-Kucera, J., Martens, D.A., van Haren, J. & Marsh, S.E. (2008) Soil carbon and nitrogen in relation to shrub size and death in a semi-arid grassland. *Geoderma*, **145**, 60–68.

Mobley, M.L., Lajtha, K., Kramer, M.G., Bacon, A.R., Heine, P.R. & Richter, D.D. (2015) Surficial gains and subsoil losses of soil carbon and nitrogen during secondary forest development. *Global Change Biology*, **21**, 986–996.

Oelofse, M., Birch-Thomsen, T., Magid, J., de Neergaard, A., van Deventer, R., Bruun, S. & Hill, T. (2016) The impact of black wattle encroachment of indigenous grasslands on soil carbon, Eastern Cape, South Africa. *Biological invasions*, **18**, 445–456.

Pacala, S.W., Hurtt, G.C., Baker, D. *et al.* (2001) Consistent land-and atmosphere-based US carbon sink estimates. *Science*, **292**, 2316–2320.

Pellegrini, A.F., Hoffmann, W.A. & Franco, A.C. (2014) Carbon accumulation and nitrogen pool recovery during transitions from savanna to forest in central Brazil. *Ecology*, **95**, 342–352.

Plotnick, R.E., Gardner, R.H., Hargrove, W.W., Prestegaard, K. & Perlmutter, M. (1996) Lacunarity analysis: a general technique for the analysis of spatial patterns. *Physical Review E*, **53**, 5461–5468.

R Development Core Team (2011) *R: A Language and Environment for Statistical Computing*. R Foundation for Statistical Computing, Vienna, Austria.

Rasse, D.P., Rumpel, C. & Dignac, M.F. (2005) Is soil carbon mostly root carbon? Mechanisms for a specific stabilisation. *Plant and Soil*, **269**, 341–356.

Ratajczak, Z., Nippert, J.B. & Collins, S.L. (2012) Woody encroachment decreases diversity across North American grasslands and savannas. *Ecology*, **93**, 697–703.

Rumpel, C. & Kögel-Knabner, I. (2011) Deep soil organic matter-a key but poorly understood component of terrestrial C cycle. *Plant and Soil*, **338**, 143–158.

Salomé, C., Nunan, N., Pouteau, V., Lerch, T.Z. & Chenu, C. (2010) Carbon dynamics in topsoil and in subsoil may be controlled by different regulatory mechanisms. *Global Change Biology*, **16**, 416–426.

Schenk, H.J. (2006) Root competition: beyond resource depletion. *Journal of Ecology*, **94**, 725–739.

Schlesinger, W.H., Raikes, J.A., Hartley, A.E. & Cross, A.F. (1996) On the spatial pattern of soil nutrients in desert ecosystems. *Ecology*, **77**, 364–374.

Schmidt, M.W., Torn, M.S., Abiven, S. *et al.* (2011) Persistence of soil organic matter as an ecosystem property. *Nature*, **478**, 49–56.

Sheldrick, B.H. & Wang, C. (1993) Particle size distribution. *Soil Sampling and Methods of Analysis, Canadian Society of Soil Science* (ed. M.R. Carter), pp. 499–511. Lewis Publishers, Ann Arbor, MI, USA.

Six, J., Conant, R.T., Paul, E.A. & Paustian, K. (2002) Stabilization mechanisms of soil organic matter: implications for C-saturation of soils. *Plant and Soil*, **241**, 155–176.

Stevens, N., Lehmann, C.E., Murphy, B.P. & Durigan, G. (2017) Savanna woody encroachment is widespread across three continents. *Global Change Biology*, **23**, 235–244.

Throop, H.L. & Archer, S.R. (2008) Shrub (*Prosopis velutina*) encroachment in a semidesert grassland: spatial-temporal changes in soil organic carbon and nitrogen pools. *Global Change Biology*, **14**, 2420–2431.

Van Auken, O.W. (2000) Shrub invasion of North American semiarid grasslands. *Annual Review of Ecology and Systematics*, **31**, 197–215.

Van Auken, O.W. (2009) Causes and consequences of woody plant encroachment into western North American grasslands. *Journal of Environmental Management*, **90**, 2931–2942.

Yang, Y., Donohue, R.J. & McVicar, T.R. (2016) Global estimation of effective plant rooting depth: implications for hydrological modeling. *Water Resources Research*, **52**, 8260–8276.

Zhou, Y., Boutton, T.W. & Wu, X.B. (2017) Data from: Soil carbon response to woody plant encroachment: importance of spatial heterogeneity and deep soil storage. *Dryad Digital Repository*, https://doi.org/10.5061/dryad.ns92q

Zhou, Y., Boutton, T.W., Wu, X.B. & Yang, C. (2017) Spatial heterogeneity of subsurface soil texture drives landscape-scale patterns of woody patches in a subtropical savanna. *Landscape Ecology*, **32**, 915–929.

Received 21 December 2016; accepted 2 March 2017
Handling Editor: Rebecca McCulley

Supporting Information

Details of electronic Supporting Information are provided below.

Fig. S1. Semivariograms for SOC density based on 320 random soil samples across this 100 m × 160 m landscape throughout the soil profile.

Fig. S2. Fine and total root biomass for different landscape elements across this 100 m × 160 m landscape throughout the soil profile.

Table S1. Summary of semivariogram model parameters for SOC density across the 100 m × 160 m landscape based on 320 random soil samples along the soil profile.

Table S2. Percentage cover (%) and mean and standard error (SE) of NDVI for different types of landscape element across this 100 m × 160 m landscape.

Table S3. Descriptive statistics for SOC density across this 100 m × 160 m landscape along the soil profile.

Appendix S1. Detailed description for variogram analysis.